

Supplemental Data

Multilineage Transcriptional Priming and Determination of Alternate Hematopoietic Cell Fates

Peter Laslo, Chauncey J. Spooner, Aryeh Warmflash, David W. Lancki, Hyun-Jun Lee, Roger Sciammas, Benjamin N. Gantner, Aaron R. Dinner, and Harinder Singh

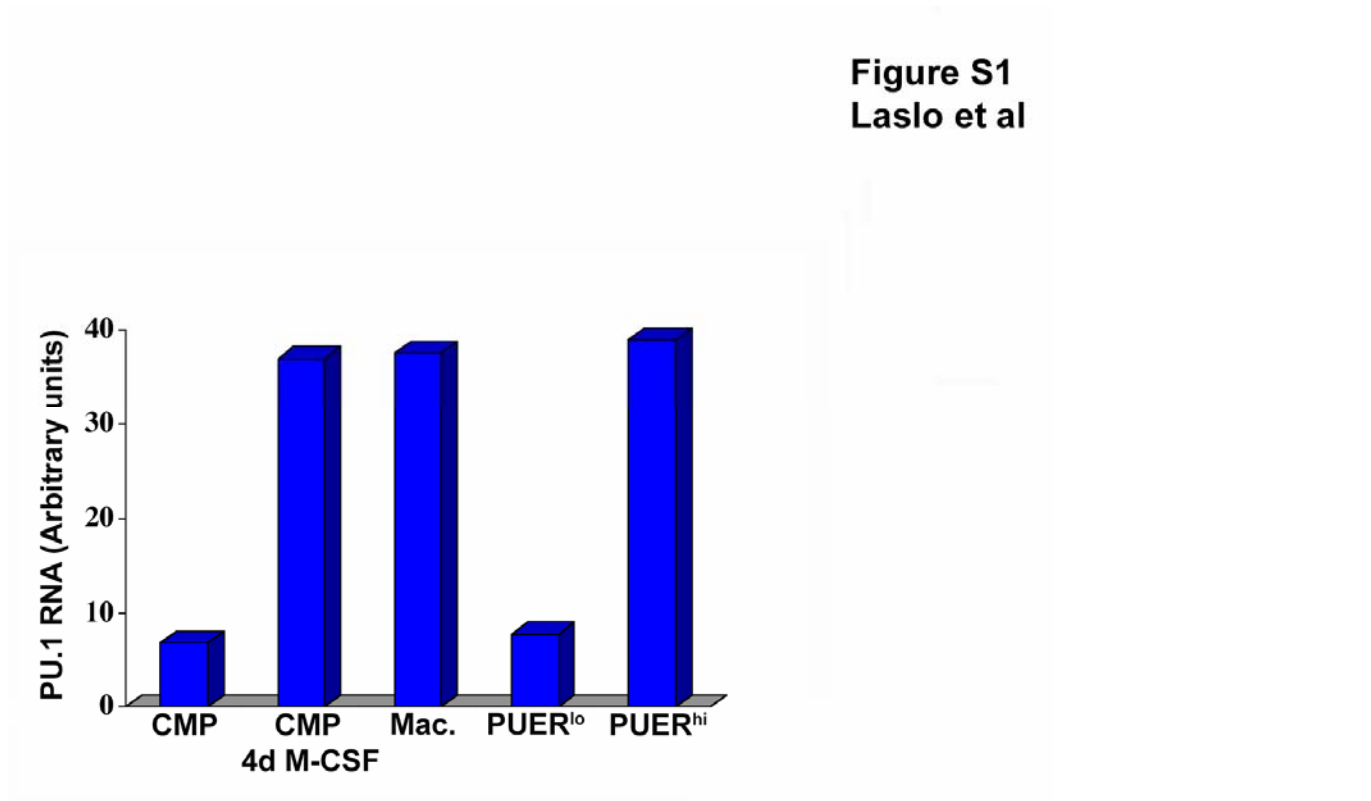


Figure S1.

Quantitative analysis of PU.1 or PUER RNA in hematopoietic progenitors and myeloid cells. PU.1 or PUER transcripts were quantitated by Q-PCR using the Mx4000 instrument (Stratagene). The various cells include CMP progenitors before and after M-CSF culture, peritoneal macrophages (Figure 1), PUER^{lo} and PUER^{hi} cells (Figure 1).

Figure S2
Laslo et al

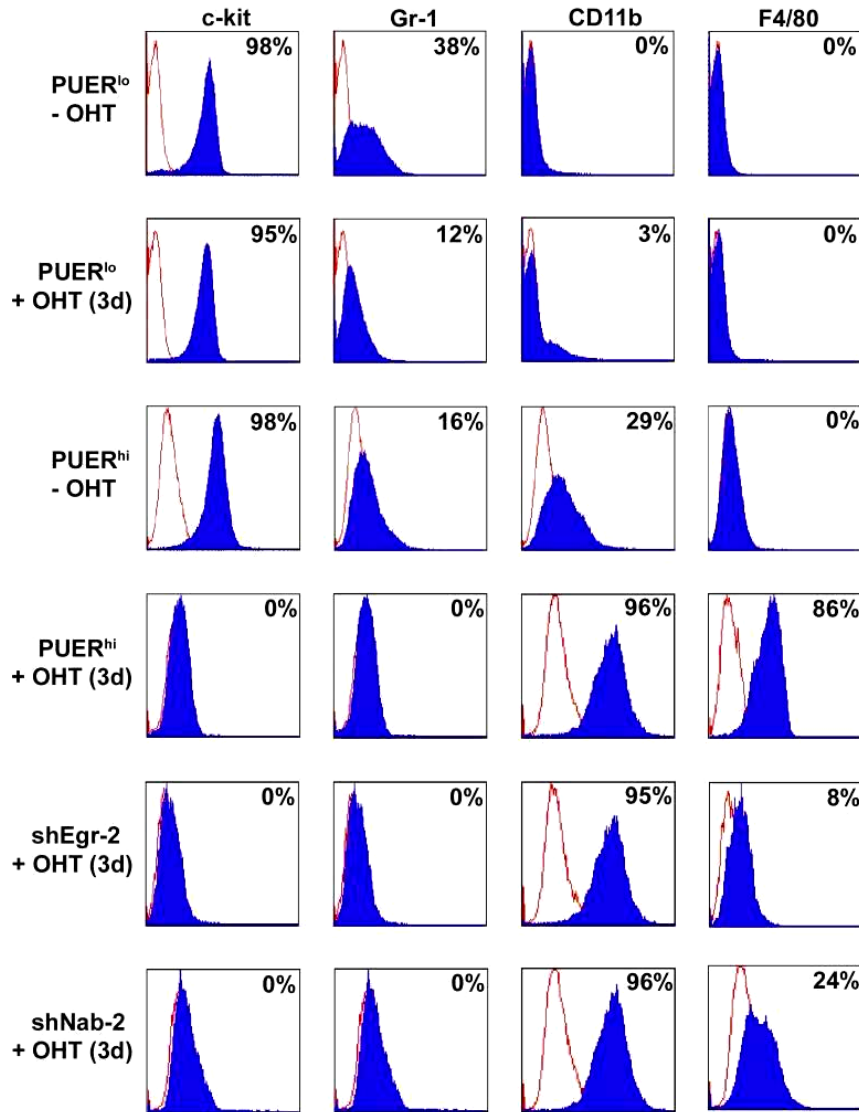


Figure S2.

Analysis of c-kit, CD11b, Gr-1 and F4/80 expression in PUER cells and their derivatives. The cells were treated with OHT (3d) and FACS analyzed. The filled and open histograms represent staining with the indicated antibody or an isotype control, respectively.

Figure S3
Laslo et al

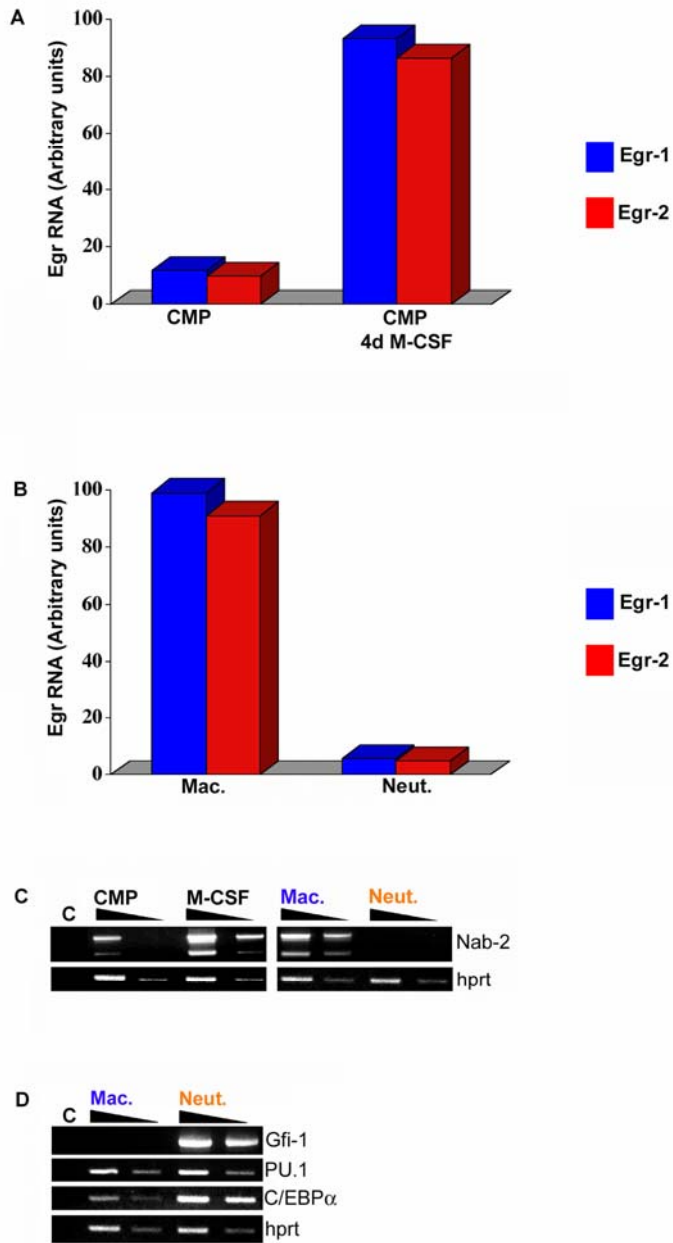


Figure S3.

(A) Quantitation of Egr-1 or Egr-2 transcripts in macrophages derived from M-CSF treated (4d) CMP progenitors by Q-PCR.

- (B) Quantitation of Egr-1 or Egr-2 transcripts in peritoneal macrophages (Mac.) and bone marrow granulocytes (Neut.; Figure 1B) as described above.
- (C) Semi-quantitative RT-PCR analysis (1:5 cDNA dilution) of Nab-2 transcripts in macrophages derived from M-CSF treated (4d) CMP progenitors (left panel) and purified peritoneal macrophages and bone marrow neutrophils (right panel).
- (D) Semi-quantitative RT-PCR analysis (1:5 cDNA dilution) of various myeloid transcription factors expressed in peritoneal macrophages and bone marrow neutrophils.

Consensus gcGTGGGcg
 Mouse (-176) caGTGGGcg
 Rat (-181) ctGGGGGat
 Human(-187) ccGGGGGct

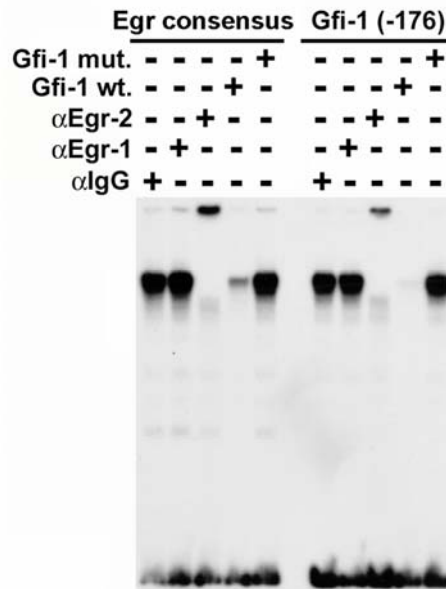


Figure S4.

Sequence comparison of the Egr site within the mouse, human and rat proximal Gfi-1 promoters (upper panel). Gel shift analysis with the Egr site in the *Gfi-1* gene (lower panel). Duplex oligonucleotides corresponding to a high affinity Egr consensus binding site or the Gfi-1 (-176) site were incubated with Egr-2 protein generated by *in vitro* translation. Protein-DNA complexes were incubated with control IgG antibody, anti-Egr-1 or anti-Egr-2 as indicated. DNA binding competition assays used either the wild type Gfi-1 or a mutant oligonucleotide as indicated.

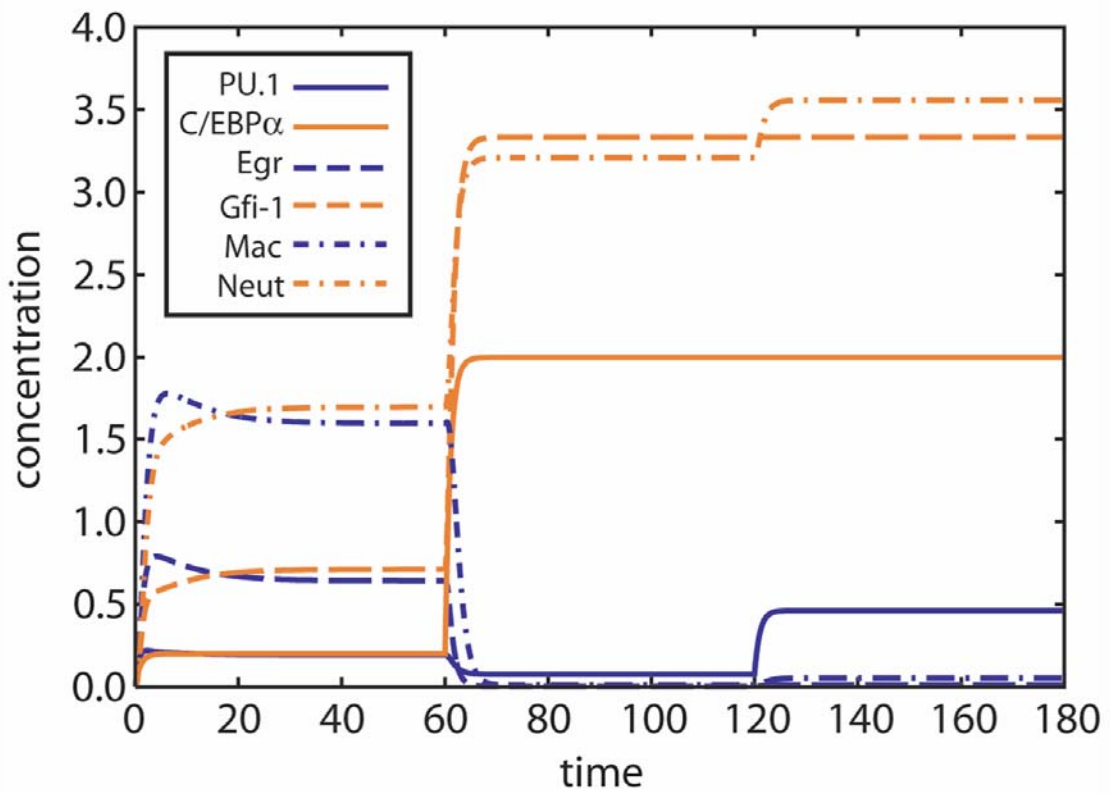


Figure S5.

Simulated experiment in which the expression of C/EBPα is increased before that of PU.1 ($t = 60$ and $t = 120$, respectively). These time series are analogous to those in Figure 6B and correspond to the previously published experiments (Dahl et al., 2003).

Figure S6
Laslo et al

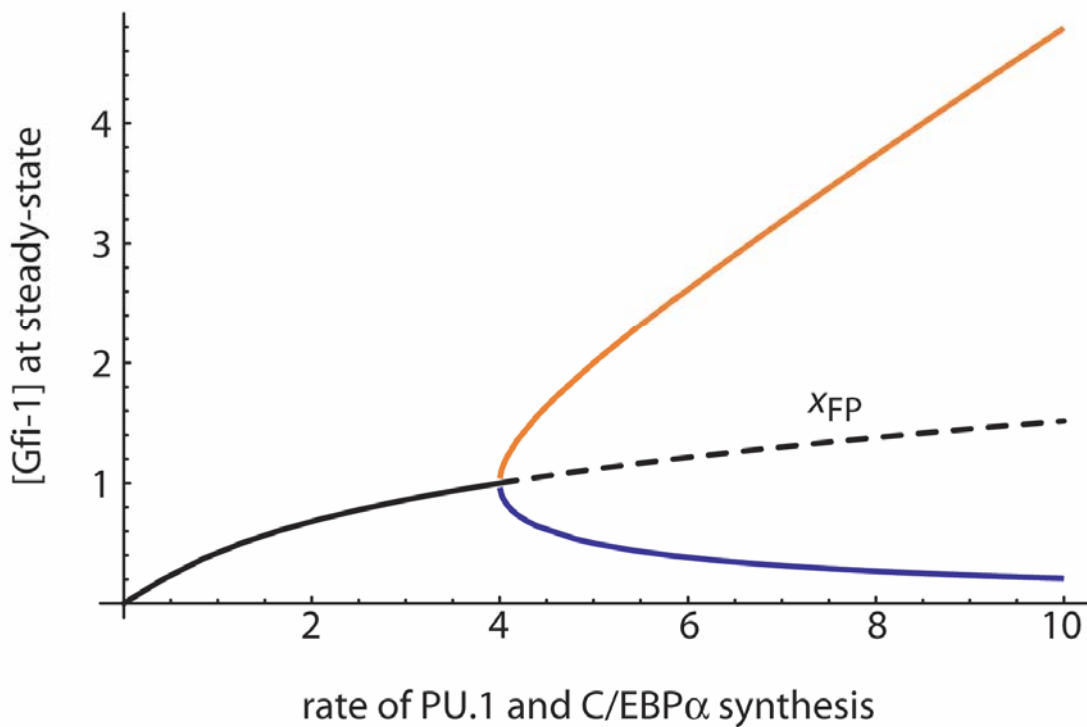


Figure S6.

Bifurcation diagram showing steady state value of Gfi-1 as a function of the rate of PU.1 and C/EBP α synthesis. The solid black line denotes the stable mixed lineage state, and the dotted black line shows the unstable mixed lineage state. The orange and blue lines correspond to the neutrophil and macrophage fixed points, respectively. See Supplemental Text for details.

Figure S7
Laslo et al

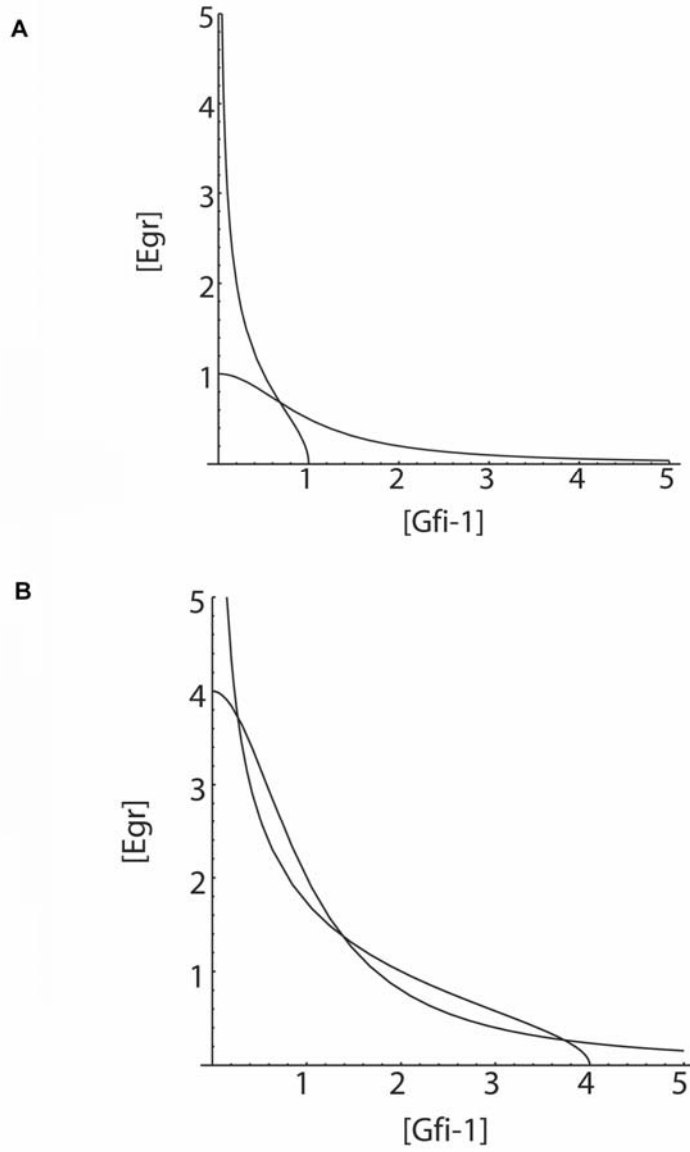


Figure S7.

Plots of the nullclines (Equation (S10)) in the N_2 - M_2 plane. In these plots, $n_R = 2$ and

(a) $C_M = C_N = 1$ or (b) $C_M = C_N = 4$.

Table S1
Laslo et al

Group 1: Examples of macrophage genes (n=99) whose induction is mutually unaffected by the knockdown of either Egr-2 or Nab-2

Gene	PUER (cont)	PUER (4d)	shEgr-2 (4d)	shNab-2 (4d)	Mac.	Neut.
Disabled 2 homologue	1,669.31	5,503.59	5,024.63	5,108.40	4,564.35	192.16
CD68	429.23	4,272.55	3,857.12	4,358.10	13,814.10	1,597.30
mmp-12	438.48	5,321.12	5,164.46	6,538.40	8,037.8	399.17
Mannosidase 1 α	1,387.83	3,928.55	3,265.50	4,258.50	3,751.7	243.55

Group 2: Examples of macrophage genes (n=3) whose induction is mis-regulated exclusively by the knockdown of Nab-2

Gene	PUER (cont)	PUER (4d)	shEgr-2 (4d)	shNab-2 (4d)	Mac.	Neut.
Nab-2	526.95	1,388.65	1,602.02	370.57	2,297.06	215.35
DNA J (Hsp40) homologue	1,236.77	3,751.65	2,902.77	1,842.70	4,313.00	908.23
cDNA sequence BC022145	343.22	2,592.37	2,213.05	607.82	5,095.78	277.87

Group3: Examples of macrophage genes (n=18) whose induction is mis-regulated exclusively by the knockdown of Egr-2

Gene	PUER (cont)	PUER (4d)	shEgr-2 (4d)	shNab-2 (4d)	Mac.	Neut.
Egr-2	201.78	4,379.94	1,710.34	3,890.60	4,407.69	204.41
c-fms	490.78	4,927.40	459.91	3,179.80	6,587.91	1,036.30
Capbactin	919.80	3,252.94	819.85	3,001.70	6,417.53	1,106.10
PCTAIRE motif-protein kinase 3	317.13	2,301.91	337.93	1,841.50	3,074.54	211.59

Group 4: Examples of macrophage genes (n=22) whose induction is mutually mis-regulated by the knockdown of either Egr-2 or Nab-2

Gene	PUER (cont)	PUER (4d)	shEgr-2 (4d)	shNab-2 (4d)	Mac.	Neut.
Cathepsin B	177.83	3,526.36	737.53	629.83	8,946.32	453.75
Fibronectin 1	346.50	4,491.07	705.30	1,163.00	5,859.49	773.36
Legumain	124.07	6,720.23	633.47	107.39	9,543.67	387.24
Phospholipid transfer protein	227.78	2,814.47	286.43	255.52	3,411.77	291.89

Table S1.

Representative examples of PU.1 induced macrophage-specific genes expressed in PUER^{hi} cells (Figure 2B) and those genes whose regulation is affected by attenuation of Egr-2 (shEgr-2 cells) or Nab-2 (shNab-2 cells). Average normalized signal intensity values for

Table S2
Laslo et al

Group 1: Examples of granulocyte genes (n=18) that are mutually mis-expressed by the knockdown of either Egr-2 or Nab-2

Gene	PUER (cont)	PUER (4d)	shEgr-2 (4d)	shNab-2 (4d)	Mac.	Neut.
Gfi-1	4,253.16	202.03	3,891.89	3,661.80	135.16	2,441.30
IL-1R (II)	192.08	471.03	3,123.52	3,087.40	232.27	5,127.20
Neutrophil elastase	13,921.10	398.10	3,251.98	3,703.50	464.07	4,419.90
Myeloperoxidase	7,770.54	767.38	11,955.95	9,506.10	282.48	7,112.99

Group 2: Examples of granulocyte genes (n=52) that are mis-expressed exclusively by the knockdown of Egr-2

Gene	PUER (cont)	PUER (4d)	shEgr-2 (4d)	shNab-2 (4d)	Mac.	Neut.
Neutrophil granule protein 2,	789.90	379.60	10,769.58	760.42	453.42	22,371.90
Stefn 2-like	377.93	286.24	5,256.85	401.97	247.69	5,796.16
mmp-8	303.10	1,901.90	6,613.01	1,919.95	350.56	14,594.20
Glutathione reductase 1	5,881.49	1,721.16	7,468.09	1,960.67	1,377.74	7,323.94

Table S2.

Representative examples of granulocyte-specific genes mis-expressed in shEgr-2 and shNab-2 cells (Figure 2D).

Supplementary Table 3
Laslo et al

EMSA Probes

Egr consensus:	TCGACTGTGTACGCGTGGGCGGTTA
Egr consensus mutant:	TCGACTGTGTACGCGTCGGCGGTTA
Gfi-1 (-176):	TCGACACTATTCCAGTGGGCGTTTCT
Gfi-1 (-176) mutant:	TCGACACTATTCCAGTCGGCGTTTCT

Table S3.

Oligonucleotide sequences used for gel shift assays (Figure S4).

Supplementary text

Isolation of primary cells

Macrophages were isolated by peritoneal lavage from mice after injection with thioglycollate medium. The cell suspension was allowed to adhere to plastic for 4d in complete IMDM medium. Non-adherent cells were removed by washing thereby yielding adherent macrophages. For isolation of neutrophils, bone marrow suspensions were stained with Ly6G-PE conjugated antibody (PharMingen) and cells sorted using MoFlo-HTS (DakoCytomation Inc.). Isolation of CMP was performed as previously described (Akashi et al., 2000). Fetal liver hematopoietic progenitors (Lin^-) were isolated from E14.5 fetuses as previously described (DeKoter et al., 1998).

Single cell RT-PCR

Multiplex single cell RT-PCR was performed as previously described with modifications (Hu et al., 1997). After FACS isolation of single cells in 96 well plates containing reverse transcription reaction components and 0.5% Triton X-100, the cell lysates was transferred into 0.25 ml eppendorf tubes and reverse transcribed with random hexamers. First round multiplex PCR amplifications were performed using one macrophage- and one neutrophil-specific primer pair. Aliquots of the first round amplification products were subjected to a second round of PCR using nested primers. Sequences of primers are available upon request.

Microarray analysis

Total RNA was isolated from peritoneal macrophages, bone marrow granulocytes, control and OHT treated (4d) PUER^{hi}, shEgr-2 and shNab-2 cells. RNAs from wild type macrophages and neutrophils were used to establish lineage specific gene expression profiles. Real time PCR was performed on select genes identified by the microarray analysis to verify their expression levels in the different cells (data not shown). Each cell sample was analyzed in duplicate. Biotin labeled cRNA was generated and hybridized to the Mouse Genome 430 2.0 Array according to manufacturer's instructions (Affymetrix). Data analyses were performed using DNA-Chip Analyzer v1.3 (Li and Wong, 2001a) with the CEL files obtained from MAS 5.0 (Affymetrix). We used a PM-only model to estimate gene expression level. The invariant set approach was used for normalization (Li and Wong, 2001b). The averaged normalized signal intensity value of each cell replicate was used for all statistical modeling.

PU.1 dependent, macrophage specific genes were identified using the following algorithm:

$$a > 3.5 * b; c > 2 * d$$

Here, a represents the normalized signal intensity for a given gene in peritoneal macrophages, b in bone marrow granulocytes, c in OHT treated PUER^{hi} cells and d in unstimulated PUER^{hi} cells. This cluster of genes was subsequently filtered to identify genes whose regulation was affected upon attenuation of either Egr-2 or Nab-2. Thus, genes were considered normally regulated, with respect to OHT treated PUER^{hi} cells, if their profile satisfied:

$$e > 0.6 * c$$

Here e represents the normalized signal intensity for a given gene in OHT treated shEgr-2 or shNab-2 cells. Insufficiently induced macrophage genes were scored as:

$$e < 0.6 * c$$

Mis-expressed granulocyte-specific genes in OHT treated shEgr-2 or shNab-2 cells were identified using the following criterion:

$$b > 3.5 * a; e > 3 * c$$

All microarray data is available upon request

Immunoblots

Immunoblots were performed as previously described (DeKoter et al., 1998) using rabbit anti-PU.1 (Santa Cruz #sc352), rabbit anti-TBP (Santa Cruz #sc225), rabbit anti-Egr-1 (Santa Cruz # sc110), rabbit anti-Egr-2 (Santa Cruz #sc190) or mouse anti-Nab-2 (kind gift from J.Milbrandt, Washington University). Protein levels between samples were estimated by serial fold dilutions of lysates.

Construction and use of small hairpin interfering RNA plasmids

Plasmids encoding shRNA oligonucleotides were constructed as described by Hannon et al (<http://www.cshl.org/public/SCIENCE/hannon.html>). Oligonucleotide sequence of the shRNA directed against Egr-2 was CCGTGCCAGAGAGATCCACACGGTGCTG. Oligonucleotide sequence of the shRNA directed against Nab-2 was CGCACAGAGCTCCCTCTCCCACAGCGGAA. The shRNA containing plasmid (pCR 2.1, Invitrogen) was further modified by sub-cloning of a pTK-Hygromycin cassette (Clontech). PUER^{hi} cells were electroporated with linear plasmid DNA and selected for

hygromycin resistance. Single cell clones (shEgr-2 or shNab-2) were isolated by limiting dilution.

Gel-Shift Assays

A putative Egr binding site was identified within the mouse *Gfi-1* promoter region (caGTGGGcg; position -176) using TRANSFAC (<http://www.gene-regulation.com/>). Egr-2 protein was generated by *in vitro* translation with a TnT coupled transcription/translation kit (Promega). DNA binding by Egr-2 was analyzed using a gel shift assay (DeKoter et al., 2002) with double stranded oligonucleotide probes containing a high-affinity Egr-2 binding site (Manzanares et al., 2002) or the Egr site located within the *Gfi-1* gene (table S3).

Chromatin Immunoprecipitation Assays

Chromatin immunoprecipitation assays were performed as previously described with slight modifications (DeKoter et al., 2002). Chromatin was incubated with anti-Egr-2 antibody (Covance # PRB-236P) or anti-Nab-2 (Santa Cruz # 12153). Sequences of primers are available upon request.

Reporter assays

For reporter assays, NIH3T3 cells were plated into 12-well plates at a concentration of 4×10^4 cells per well and cultured overnight. Cells were transfected the following day with 100 ng of luciferase reporter, 1ng of CMV-driven *Renilla* reporter, indicated amounts of Egr-2, Nab-2, Gfi-1 and Gfi-1 (P2A) expression plasmid and pBluescript as required to

make a total of 1 ug DNA per well using the Fugene transfection reagent (Roche). After 48hr, cells were washed, lysed and levels of both firefly and *Renilla* luciferase activities measured using a dual luciferase assay kit (Promega). All transfections were performed in triplicates at least three independent times. The Egr-2 and Nab-2 expression constructs were a kind gift from J. Svaren, University of Wisconsin while the Gfi-1 and Gfi-1 (P2A) plasmids were gift from R. Dahl, University of New Mexico.

Mathematical model of gene regulatory network

The time evolution of the molecular populations is determined by a set of ordinary differential equations. As discussed in the main text, many of the transcription factor binding sites of the regulatory network are known, but the consequences of their occupancy are not understood in quantitative detail. Consequently, we take a general form for the rate laws, similar to ones employed in earlier theoretical treatments of gene expression (Gardner et al., 2000; Angeli et al., 2004; Elowitz and Leibler, 2000; Ozbudak et al., 2004; Acar et al., 2005). The concentration of each protein (x) varies as

$$\frac{dx}{dt} = \left(\frac{\alpha A^{n_A}}{K_A^{n_A} + A^{n_A}} + e_0 \right) \frac{K_R^{n_R}}{K_R^{n_R} + R^{n_R}} - \beta x \quad (\text{S1})$$

where A is the concentration of activator, R is the concentration of repressor, n_R and n_A , are Hill coefficients for repression and activation, K_R and K_A are the half saturation constants for repression and activation, α is the maximum rate of protein production caused by the activator, β is the rate of protein degradation, and e_0 is the rate of protein synthesis in the absence of activator. In the case that a gene is not regulated, we set $A = 0$ and $R = 0$ on the righthand side of Equation (S1). The term e_0 is included to avoid

extending the network to include activators for the primary cell fate determinants; $e_0 > 0$ for PU.1 and C/EBP α , and $e_0 = 0$ for all other genes.

If we assume that $K=K_R=K_A$ and β are the same for all species, we are free to rescale the protein concentrations and time by these parameters, respectively. In other words, the units of protein concentration are such that $K = 1$, and the units of time are such that $\beta=1$. Denoting the primary genes PU.1 and C/EBP α by M_1 and N_1 , respectively, and the secondary genes Egr and Gfi-1 by M_2 and N_2 , respectively, this choice of units leads for the macrophage genes to the equations:

$$\frac{dM_1}{dt} = \frac{e_M}{1 + N_2^{n_R}} - M_1 \quad (\text{S2a})$$

$$\frac{dM_2}{dt} = \left[\frac{\alpha M_1^{n_A}}{1 + M_1^{n_A}} \right] \frac{1}{1 + N_2^{n_R}} - M_2. \quad (\text{S2b})$$

For the expression of C/EBP α ,

$$\frac{dN_1}{dt} = e_N - N_1. \quad (\text{S2a}')$$

The equation for Gfi-1 is obtained by swapping M and N in Equation (S2b). Unless otherwise specified, we assume activation follows Michaelis-Menten-like kinetics ($n_A = 1$) and repression is cooperative ($n_R = 4$). We take $\alpha = 5$, which corresponds to a maximum steady-state expression level that is five times the half saturation value (K).

Because each of the downstream genes (represented by Mac and Neut in Figure 6A and denoted M_3 and N_3 below) has multiple activators, a more general form is required. We base our choice on recent data for the regulation of *c-fms*, a macrophage specific gene which acts downstream of Egr-2 (H. Krysinska and C. Bonifer, personal communication). Activation of this gene is a two-step process. Initially, PU.1 and

C/EBP α bind to the promoter region and activate transcription at low levels. Expression of PU.1 also leads to transcription of Egr-2, which binds with much slower kinetics to an additional regulatory element known as FIRE and fully activates the *c-fms* gene. Based on these observations and earlier ones (Smith et al., 1996; Zhang et al., 1996), we take the expression of the downstream macrophage genes to be

$$\frac{dM_3}{dt} = \left(\frac{\alpha_{lo} M_1 N_1}{1 + M_1 N_1} + \frac{\alpha_{hi} M_2}{1 + M_2} \right) \frac{1}{1 + N_2^{n_R}} - M_3. \quad (\text{S2c})$$

Here, the first term in parentheses describes the synergistic action of PU.1 and C/EBP α bound to the *c-fms* promoter, and the second term describes the transcription due to Egr-2 binding to FIRE ($\alpha_{lo} = 1$ and $\alpha_{hi} = 4$). Although there are in fact multiple PU.1 binding sites in the promoter, M_1 was not raised to a higher power because the quantitative consequences of more than one PU.1 molecule binding at a time are unknown. An analogous equation with M and N swapped is used for N_3 . It is important to stress that the tertiary determinants do not affect the dynamics of the upstream genes and thus function only as readouts in our model. Consequently, the qualitative conclusions we present are robust to alternative forms for Equation (S2c) and the choice of units discussed above.

To obtain the results presented in the main text and in Figure S5, the differential equations in Equation (S2) were integrated using a fourth order Runge-Kutta algorithm (Press et al., 1992). Use of ordinary differential equations ignores stochastic fluctuations in protein concentrations, which are inherent in biological systems. However, cell fates are determined over long times in comparison with molecular fluctuations. Addition of noise does not change the number of stable states or perturb the behavior of the system

qualitatively when it is in a stable state (data not shown). However, it does allow cells close to the separatrix to partition naturally into macrophages and neutrophils during the transition from monostability to bistability. A very similar model was used by Gardner et al. (2000) to model a bistable gene regulatory switch.

Steady-state analysis

The observable cell fates are those that correspond to stable steady states ($dx/dt = 0$ for $x = M_1, M_2, M_3, N_1, N_2,$ and N_3). In the following supplemental analysis, we neglect the feedback from Gfi-1 to PU.1 (making the M_1 equation identical in form to the N_1 one), which allows us to obtain a number of results analytically by exploiting symmetry properties of the resulting network. Setting the lefthand sides to zero in Equation (S2), we obtain from the primary factor equation $M_1 = e_M$. Defining $C_M = \frac{\alpha M_1^{n_A}}{1 + M_1^{n_A}} = \frac{\alpha e_M^{n_A}}{1 + e_M^{n_A}}$ and similarly for C_N , the steady-state concentrations of the secondary factors are determined by the equations:

$$M_2 = \frac{C_M}{1 + N_2^{n_R}} \quad (\text{S3a})$$

$$N_2 = \frac{C_N}{1 + M_2^{n_R}}. \quad (\text{S3b})$$

Given M_2 and N_2 , the steady-state concentrations of the downstream elements follow immediately from Equation (S2c). Consequently, the number of (stable and unstable) fixed points of the system described by the ordinary differential equations depends on the

number of physically meaningful solutions of Equation (S3), which, in turn, depends on the values of C_M , C_N , and n_R .

In the case that $e_M = e_N$ (so $C_M = C_N = C$), symmetry considerations indicate that there is always a solution with

$$M_2 = N_2 = x_{\text{FP}} = \frac{C}{1 + x_{\text{FP}}^{n_R}}. \quad (\text{S4})$$

where x_{FP} is defined by the above equation. To evaluate the stability of this fixed point, we restrict our attention to the secondary factors. The Jacobian in the reduced space is

$$J = \begin{pmatrix} -1 & -\frac{Cn_R N_2^{n_R-1}}{(1 + N_2^{n_R})^2} \\ -\frac{Cn_R M_2^{n_R-1}}{(1 + M_2^{n_R})^2} & -1 \end{pmatrix} \quad (\text{S5})$$

with eigenvalues evaluated at x_{FP}

$$\lambda_{\pm} = -1 \pm \frac{n_R x_{\text{FP}}^{n_R}}{1 + x_{\text{FP}}^{n_R}}. \quad (\text{S6})$$

For the mixed lineage state to be stable, both eigenvalues must be negative, which is the case when $(n_R - 1)x_{\text{FP}}^{n_R} < 1$. In particular, for $n_R = 1$, the inequality is always satisfied, and the system never bifurcates into stable macrophage and neutrophil (and unstable mixed) lineages. For $n_R > 1$, transition to the differentiated states occurs as the expression levels of the primary factors increase because x_{FP} increases with e_M and e_N . As n_R and α increase (more cooperative repression or more responsive activation, respectively), the bistable (differentiated) regime grows and the monostable (mixed lineage) regime diminishes. Gardner et al. (2000) show similar behavior for changes in α .

Macrophage and neutrophil lineage fixed points for $n_R = 2$

For the special case of $n_R = 2$, it is also straightforward to determine the values of the other fixed points in the bistable regime. We use Equation (S3b) to write N_2 in terms of M_2 and substitute this result into Equation (S3a). We then multiply out the resulting equation to obtain a fifth order polynomial. We can factor out the symmetric solution (Equation (S4)) from this polynomial:

$$\begin{aligned} 0 &= M_2^5 - CM_2^4 + 2M_2^3 - 2CM_2^2 + (1 + C^2)M_2 - C \\ &= (M_2^3 + M_2 - C)(M_2^2 - CM_2 + 1) \end{aligned} \quad (\text{S7})$$

The solutions to the quadratic part are:

$$M_2 = \frac{C \pm \sqrt{C^2 - 4}}{2}. \quad (\text{S8})$$

By symmetry,

$$N_2 = \frac{C \mp \sqrt{C^2 - 4}}{2}. \quad (\text{S9})$$

Real, positive solutions for $M_1 \neq N_2$ thus exist for $C > 2$. In other words, for sufficiently high expression of the primary factors (which enter through C), there are simultaneous macrophage (Egr^{hi} and Gfi^{lo}) and neutrophil (Egr^{lo} and Gfi^{hi}) solutions. By substituting M_1 and N_2 into Equation (S5), it can be shown that these states are always stable (the real parts of both eigenvalues of the Jacobian are negative). The stability condition for the mixed lineage fixed point reduces to $x_{\text{FP}} < 1$ for $n_R = 2$, and this inequality is never satisfied when $C > 2$. These considerations are summarized in the pitchfork bifurcation diagram in Figure S6.

The behavior is qualitatively similar for the more general situation when the rates of synthesis e_M and e_N are not equal and $n_R > 1$, but it is necessary to solve for the number

of roots numerically. In the main text, we consider $n_R = 4$. Although $n_R = 2$ was sufficient to capture the features of interest in the present work, greater cooperativity is required to account for observations in lineage reprogramming experiments (Xie et al., 2004) (AW, HS and ARD, in preparation).

Analytic phase diagram

The boundary between the monostable and bistable regimes can be obtained from solution of a system of equations, rather than numerically evaluating the number of solutions to Equation (S3). First, we invert the second equation in Equation (S3) so that we have two equations for M_2 in terms of N_2

$$M_2 = \frac{C_M}{1 + N_2^{n_R}} \text{ and } M_2 = \left(\frac{C_N}{N_2} - 1 \right)^{\frac{1}{n_R}} \quad (\text{S10})$$

If we plot these equations in M_2 - N_2 plane (Figure S7), the two curves intersect either once (monostable) or three times (two stable and one unstable fixed points). The boundary between these regimes will be where these two curves are tangent to one another. Thus by equating the two expressions for M_2 and the resulting expressions obtained by differentiating with respect to N_2 , we obtain two conditions:

$$\frac{C_M}{1 + N_2^{n_R}} = \left(\frac{C_N}{N_2} - 1 \right)^{\frac{1}{n_R}} \text{ and } \frac{C_M n_R N_2^{n_R-1}}{(1 + N_2^{n_R})^2} = \frac{C_N}{N_2 n_R} \left(\frac{C_N}{N_2} - 1 \right)^{\frac{1}{n_R}-1}. \quad (\text{S11})$$

One of these equations can be used to eliminate N_2 and thus we have an expression for the boundary of the bistable regime. For $n_R = 2$, this system of equations can be solved and the resulting phase plane diagram is similar to Figure 6C of the main text.

Supplementary References

- Acar, M., Becskei, A., and van Oudenaarden, A. (2005). Enhancement of cellular memory by reducing stochastic transitions. *Nature* *435*, 228-232.
- Akashi, K., Traver, D., Miyamoto, T., and Weissman, I. L. (2000). A clonogenic common myeloid progenitor that gives rise to all myeloid lineages. *Nature* *404*, 193-197.
- Angeli, D., Ferrell, J. E., Jr., and Sontag, E. D. (2004). Detection of multistability, bifurcations, and hysteresis in a large class of biological positive-feedback systems. *Proc Natl Acad Sci U S A* *101*, 1822-1827.
- DeKoter, R. P., Walsh, J. C., and Singh, H. (1998). PU.1 regulates both cytokine-dependent proliferation and differentiation of granulocyte/macrophage progenitors. *Embo J* *17*, 4456-4468.
- DeKoter, R. P., Lee, H. J., and Singh, H. (2002). PU.1 regulates expression of the interleukin-7 receptor in lymphoid progenitors. *Immunity* *16*, 297-309.
- Elowitz, M. B., and Leibler, S. (2000). A synthetic oscillatory network of transcriptional regulators. *Nature* *403*, 335-338.
- Gardner, T. S., Cantor, C. R., and Collins, J. J. (2000). Construction of a genetic toggle switch in *Escherichia coli*. *Nature* *403*, 339-342.
- Hu, M., Krause, D., Greaves, M., Sharkis, S., Dexter, M., Heyworth, C., and Enver, T. (1997). Multilineage gene expression precedes commitment in the hemopoietic system. *Genes Dev* *11*, 774-785.
- Li, C., and Wong, W. H. (2001a). Model-based analysis of oligonucleotide arrays: expression index computation and outlier detection. *Proc Natl Acad Sci U S A* *98*, 31-36.
- Li, C., and Wong, W. H. (2001b). Model-based analysis of oligonucleotide arrays: model validation, design issues and standard error application. *Genome Biology* *2*, 32.31-32.11.
- Manzanares, M., Nardelli, J., Gilardi-Hebenstreit, P., Marshall, H., Giudicelli, F., Martinez-Pastor, M. T., Krumlauf, R., and Charnay, P. (2002). Krox20 and kreisler cooperate in the transcriptional control of segmental expression of Hoxb3 in the developing hindbrain. *Embo J* *21*, 365-376.
- Ozbudak, E. M., Thattai, M., Lim, H. N., Shraiman, B. I., and Van Oudenaarden, A. (2004). Multistability in the lactose utilization network of *Escherichia coli*. *Nature* *427*, 72-75.
- Press, W. H., Teukolsky, S. A., Vetterling, W. T., and Flannery, B. P. (1992). *Numerical Recipes in C*. (New York: Cambridge University Press)

Smith, L. T., Hohaus, S., Gonzalez, D. A., Dziennis, S. E., and Tenen, D. G. (1996). PU.1 (Spi-1) and C/EBP alpha regulate the granulocyte colony-stimulating factor receptor promoter in myeloid cells. *Blood* 88, 1234-1247.

Xie, H., Ye, M., Feng, R., and Graf, T. (2004). Stepwise reprogramming of B cells into macrophages. *Cell* 117, 663-676.

Zhang, D. E., Hetherington, C. J., Meyers, S., Rhoades, K. L., Larson, C. J., Chen, H. M., Hiebert, S. W., and Tenen, D. G. (1996). CCAAT enhancer-binding protein (C/EBP) and AML1 (CBF alpha2) synergistically activate the macrophage colony-stimulating factor receptor promoter. *Mol Cell Biol* 16, 1231-1240.